SMALL ANGLE X-RAY SCATTERING STUDIES OF PHASE TRANSITIONS IN POLYMERIC AND OLIGOMERIC SYSTEMS

E. W. FISCHER

Institut für Physikalische Chemie der Universität Mainz, II. Ordinariat, Mainz, Germany

ABSTRACT

Small angle x-ray scattering (SAXS) is a valuable method for studying structure changes which take place during phase transitions in polymeric and oligomeric systems. Measurements of the dependence of SAXS on temperature yield information on the changes in morphology or of the structure on a supermolecular level. The technique can be applied to various problems: glass transition in highly crystalline polymers, solid state phase transitions in crystalline polymers, rotational transition in *n*-paraffins, premelting phenomena in crystals of chain molecules, and partial melting of homo- and co-polymers.

The glass transition temperature of the amorphous regions in highly crystalline polymers can be measured by SAXS since the scattered intensity depends on the thermal expansion coefficient of the two phases. This technique was applied to so-called single crystals grown from solution of polybutene-1, branched and linear polyethylene. The amorphous surface layer of linear polyethylene single crystals exhibits a T_g of $-125° \pm 4°C$.

Solid state phase transitions of polymer crystals are often accompanied by characteristic changes in morphology. As examples, the annealing behaviour of *trans*-1,4-polybutadiene and isotactic polybutene-1 is described.

The 'rotational' transition in paraffins studied with *n*-tritriacontane as an example also leads to a pronounced structure change of the surface of the paraffin lamellae, speaking in favour of a transition theory which is based on the assumption of a sudden change in the concentration of kinks within the crystals.

With increasing temperature an increase of the roughness and depth of the surface region of paraffin crystals is observed. This phenomenon can be described as 'surface premelting of chain molecular crystals' and SAXS yields quantities suitable for a thermodynamic explanation of that process.

In homo- and co-polymer crystals partial melting during heating is observed. The SAXS studies show that this effect can be due to a 'boundary premelting of polymer crystals' which manifests itself by a reversible increase of the thickness of the intercrystalline layers. This phenomenon can be observed in many polymers, it can be described quantitatively by analysis either of the scattering curves or of the correlation functions $\gamma(x)$ obtained from the intensity distribution.

1. INTRODUCTION

In physics and chemistry we are well acquainted with a wide variety of phenomena which are characterized by drastic changes in physical properties resulting from changes in temperature. These are called phase transitions and show many similarities at a macroscopic level. At this level they are quite well understood and the thermodynamics of phase transitions supplies a sound framework for the description of such phenomena.

On the other hand we must not expect that either a macroscopic theory or methods yielding macroscopic quantities will lead us to a more far-reaching understanding of the processes causing the various phase transitions. An explanation of these phenomena can be expected only in terms of structural changes, whereas thermodynamics can ignore completely the structure of the states of matter treated. Consequently some of the most important general conclusions about melting and crystallization were reached even before the atomic structure of matter was generally accepted[1], but it was the introduction of the powerful method of x-ray diffraction which led to a tremendous increase in the understanding of the nature of phase transitions.

In many cases, however, it turned out that the picture revealed by x-ray wide angle diffraction provides only a partial answer to the question: How does the structure change during a phase transition? This point may be demonstrated by looking at the melting behaviour of a partially crystalline polymer as an example. From x-ray diffraction experiments it is known only that melting is associated with the disappearance of long range order in the packing of the chain molecules. The accompanying change of structure can be visualized as shown in *Figure 1*[1]. This explanation for the change of

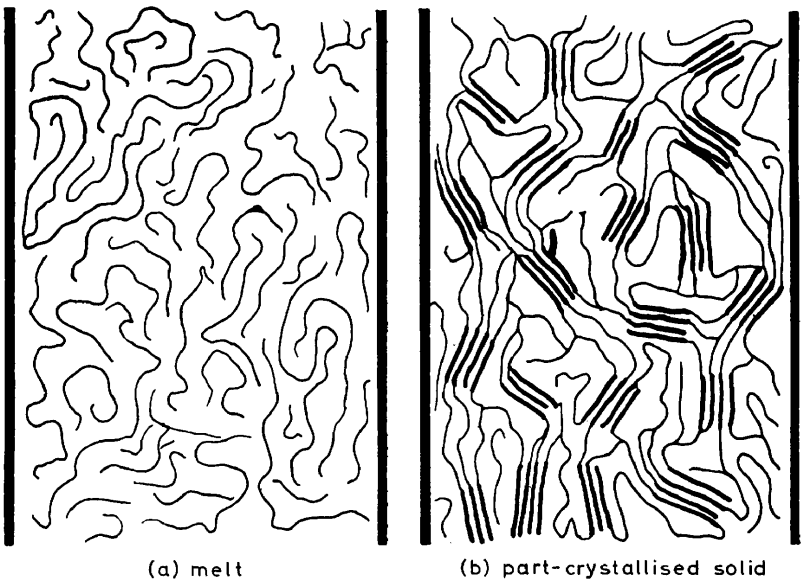

Figure 1. Model of the changes in structure during melting and crystallization of polymers (after A. R. Ubbelohde[1]).

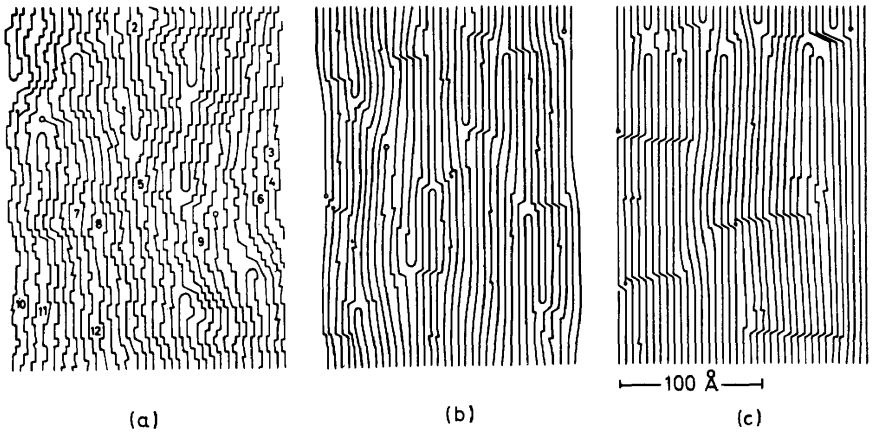

Figure 2. Suggested models of various states of polyethylene: (a) in the melt, (b) in the solid state at temperatures near the melting point, (c) in the solid state at low temperatures (after W. Pechhold and S. Blasenbrey[2]).

molecular conformation is based on models of the partly crystalline solid and of the polymer melt and it has been accepted for a long time by many workers in this field. A quite different model of melting[2,3] is shown in *Figure 2*. Melting is supposed to result from a sudden change in the concentration of a special type of conformation defect ('kinks') at the melting point.

One of the main differences between the two models presented here can be described in terms of 'morphology' or 'supermolecular order'. For the investigation of this type of structure one has to look for other experimental methods in addition to x-ray wide angle diffraction. Information about structures on a supermolecular scale is obtained especially by electron microscopy and small angle x-ray scattering (SAXS). These methods have been applied extensively to the investigation of both the structure of the solid crystalline polymer and the melt or 'amorphous' polymer. The results of these studies have to be taken into account when considering theories of melting and crystallization of polymers.

Besides the example mentioned above, there exist many other problems regarding phase transitions in polymeric and oligomeric systems where SAXS can provide indispensable information about structure changes on a supermolecular level with dimensions in the range between 10 Å and some thousand Å. The principle of a scattering apparatus often used is shown in *Figure 3*(a)[4]. As an example of a scattering curve, the intensity versus the scattering angle is plotted in *Figure 3*(b) for a mat of polyethylene single crystals grown from dilute solution[5]. From the absolute value of the scattered intensity, the magnitude of the fluctuation of the electron density can be revealed. The shape of the curve and the position of the intensity peaks yield quantities related to the spatial arrangement of the density fluctuations. Therefore SAXS can supply useful information about phase transitions if these processes are accompanied either by changes in magnitude of the fluctuation or by changes in the geometry of the scattering system.

In the following paper I want to demonstrate some applications of the SAXS technique to transition problems in systems consisting of linear chain molecules. After a short review of the basic methods for analysing the

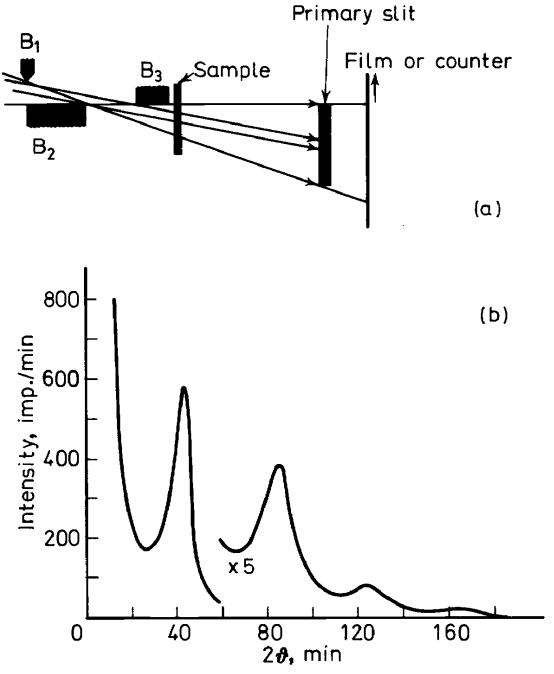

Figure 3. (a) Schematic drawing of a small angle x-ray scattering camera with slit collimation (after O. Kratky[4]). (b) SAXS curve of a mat of polyethylene single crystals grown from dilute solutions[5].

scattering pattern we will treat the glass transition in highly crystalline polymers as an example where the dependence of electron density fluctuation on temperature can be measured by SAXS. The next section will deal with the changes in morphological structure due to solid-state phase transitions in polymers. Subsequently SAXS investigations on the order–disorder transitions in *n*-paraffins will be considered. Finally the application of SAXS to the problems of partial melting and premelting effects in polymers will be treated.

2. ANALYSIS OF SMALL ANGLE X-RAY DIFFRACTION CURVES

The theory of SAXS has been treated by many investigators such as Porod, Kratky, Debye, Hosemann, Guinier, Luzatti, Bonart, Peterlin and other distinguished authors. For literature we refer to a recent review article by Hosemann *et al.*[6] and to a bibliography by A. J. Renouprez[7]. There are different approaches for analysing the scattering behaviour of a sample. The greatest difference arises from the distinction between 'dilute' and 'dense'

systems. In the first case the small angle scattering pattern can be considered simply as the sum of the scattering patterns of the individual particles contained in the scattering volume. Then the scattered intensity generally decreases continuously with scattering angle and the analysis is based on evaluation of the scattering by a single particle.

The theoretical treatment is more complicated however, if interparticular interference has to be taken into account, as is the case, for example, in a densely packed system of crystallites in a solid polymer. Very often one obtains distinct 'long spacing' reflection due to such interference and consequently the scattering system is treated as a superlattice with distorted periodicity.

There are two ways of analysing the SAXS curves of densely packed systems. The most general information about the structure of the scattering sample can be obtained by inverse Fourier transformation of the intensity distribution $S_0(\mathbf{b})$:

$$\begin{aligned} Q(\mathbf{x}) &= \mathscr{F}^{-1}[S_0(\mathbf{b})] \\ &= \int_{\infty}\int\int S_0(\mathbf{b}) \exp(2\pi i \mathbf{b}\mathbf{x})\, \mathrm{d}b_1 \mathrm{d}b_2 \mathrm{d}b_3 \end{aligned} \tag{1}$$

where

$$\mathbf{b} = (\mathbf{s} - \mathbf{s}_0)/\lambda\,; |b| = 2 \sin \vartheta/\lambda \tag{2}$$

$\mathbf{b}$ is the vector in reciprocal space with orthogonal components b_1, b_2, b_3. s_0 and $\mathbf{s}$ are unit vectors in the directions of the primary and scattered beams respectively, and $2\,\vartheta$ is the scattering angle. The intensity distribution $S_0(\mathbf{b})$ in reciprocal space can be evaluated from the measured scattering curves $J(\vartheta)$ by application of the usual correction procedures including the slit-pinhole correction process (see below).

The Q-function of equation 1 introduced by Hosemann[8] is the convolution square of the electron density

$$Q(\mathbf{x}) = \int_{\infty}\int\int \rho(\mathbf{x} + \mathbf{y})\, \rho(\mathbf{y})\, \mathrm{d}y_1 \mathrm{d}y_2 \mathrm{d}y_3 \tag{3}$$

and is related to the correlation function $\gamma(\mathbf{x})$ defined by Debye and Bueche[9]

$$\gamma(\mathbf{x}) = \lim_{V_y \to \infty} \frac{\int_{V_y}\int\int \eta(\mathbf{x} + \mathbf{y})\, \eta(\mathbf{y})\, \mathrm{d}^3 y}{\int_{V_y}\int\int \eta^2(\mathbf{y})\, \mathrm{d}^3 y} \tag{4}$$

where $\eta(\mathbf{x})$ is the density fluctuation

$$\eta(\mathbf{x}) = \rho(\mathbf{x}) - \langle \rho \rangle \tag{5}$$

within the sample. If only the observable part of the Q-function is considered, the inverse Fourier-transformation of the corrected 'pinhole' scattering curve $S_0(b)$ yields the space average of the convolution square of the electron fluctuation $\eta(\mathbf{x})$, see reference 6. Thus one may analyse the SAXS pattern by calculating the Q-function of a density distribution for a model and comparing this result with the Q-function computed from the measured data. Some very

important integral parameters of the model can be obtained immediately from the measured correlation function as we will see later.

A second way of analysing the scattering behaviour of the sample is the calculation of scattering functions of model systems and comparing these with the measured curves. It may often be suitable to regard the sample as a paracrystalline superlattice, where each brick (crystallite) consists of several thousand atoms. This treatment can be justified by electron microscopical observations. The scattering theory of a paracrystal developed by Hosemann[8] yields the scattering function

$$S_0(\mathbf{b}) = N[\langle B^2\rangle - \langle B\rangle^2] + \frac{\langle B\rangle^2}{V}(Z(\mathbf{b}) * |S(\mathbf{b})|^2) \tag{6}$$

where $B(\mathbf{b})$ is the scattering factor of a single brick of the superlattice; $Z(\mathbf{b})$ is the paracrystalline lattice factor obtained by Fourier transformation of the lattice statistics; and $S(\mathbf{b})$ is the shape factor of the superlattice.

The calculated scattering functions can be compared with the measured intensity curves. Using this procedure one can estimate rather easily the value of the long spacing, i.e. the average distance of the bricks in the superlattice, and the fluctuation of the distances.

Both methods can be used so that it depends on the information required and on the knowledge available about the systems which way is preferred. There is one important quantity obtained from the Q-function for $x = 0$. According to equations 3 and 5 the observable part of the Q-function yields

$$Q_{\text{observ.}}(0) = \int \eta(\mathbf{y})\,\eta(\mathbf{y})\,\mathrm{d}^3\mathbf{y} = \langle \eta^2\rangle\, V \tag{7}$$

This quantity is the scattering power of the sample and is proportional to the average square density fluctuation. It does not depend on the shape of the Q-function; that means it is independent of the geometrical arrangement of the scattering units. There is a simple relation between $\langle \eta^2\rangle$ and the composition of a two-phase model

$$\langle \eta^2\rangle = (\rho_1 - \rho_2)^2\, w_1 w_2 \tag{8}$$

where $\rho_{1,2}$ are the densities of the two phases and $w_{1,2}$ their volume fractions. The scattering power can be calculated if the scattered intensity is measured on an absolute scale according to equation 1

$$\langle \eta^2\rangle = \frac{\text{const}}{J_0}\int S_0(\mathbf{b})\,\mathrm{d}^3\mathbf{b} \tag{9}$$

where J_0 is the primary intensity.

Another integral parameter of the scattering system can be determined from the slope of the correlation function $\gamma(x)$ at $x = 0$. For a two-phase structure one obtains the specific internal surface[9, 10]

$$Q/V \sim \gamma'(0) \tag{10}$$

So far the methods of analysis are based on scattering curves $S_0(\mathbf{b})$ obtained by a primary beam of pointlike cross section which can be realized by collimating the beam by very small pinholes. For intensity reasons a slit collimation system is often used, however, and the experimental result is a

slit-smeared scattering curve. Many methods have been proposed for evaluating the slit corrected data; we used a technique recently developed in our institute by G. R. Strobl[11] which is applicable to any primary beam intensity distribution. In addition it yields directly the correlation function

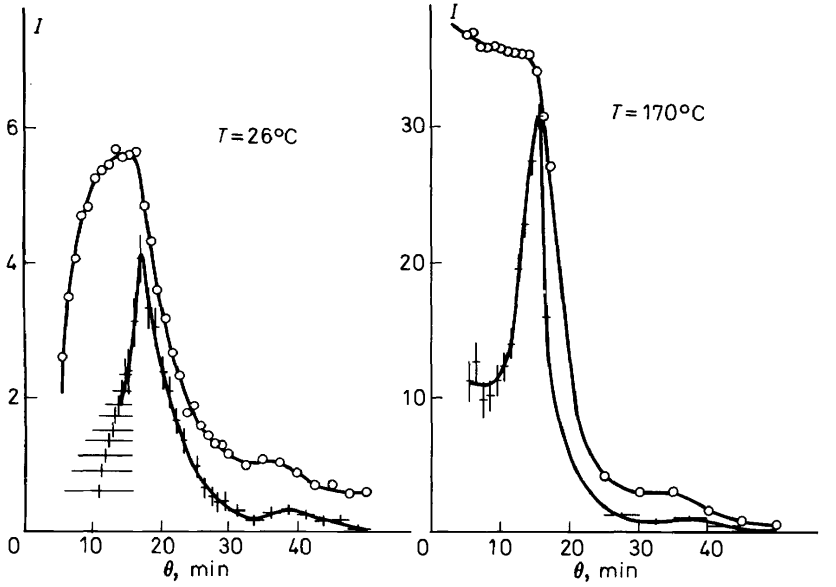

Figure 4. Examples of changes in SAXS curves by use of slit-correction: -O-O- measured intensity -+-+- corrected pinhole scattering curve, the bars indicate the statistical confidence regions of the calculated data. Scattering curves were obtained from melt crystallized polyoxymethylene measured at the indicated temperatures[57].

and values characterizing the precision of the calculated quantities. As an example *Figure 4* shows two scattering curves of polyoxymethylene and the calculated pinhole curves.

3. STUDIES OF GLASS TRANSITION IN HIGHLY CRYSTALLINE POLYMERS

When discussing the application of the SAXS technique to transition problems in the polymer field, we start with the phenomenon of the glass transition, although it is well known that a number of eminent investigators concluded from their measurements or from theoretical considerations that the glass transition in polymers cannot properly be classified as a true higher order transition in the thermodynamic sense. We are not concerned with this problem, however, but rather with the problem regarding the determination of the glass transition temperature in highly crystalline polymers and with the conclusions which can be drawn from our measurements with regard to the structure of the 'amorphous' phase in such polymers.

The main experimental difficulty in measuring the glass transition

phenomenon in highly crystalline polymers arises from the proportionality between the magnitude of the measured effect and the fraction of amorphous material present in the sample. Therefore for a high degree of crystallinity, the changes in specific volume or specific heat due to the glass transition in the minor amorphous component are rather small. For the same reason the glass transition often cannot be detected in tan δ measurements or in the second moment of the n.m.r. absorption spectra. In contrast to this the SAXS technique yields a valuable tool for studying glass transitions in highly crystalline polymers.

The foundation of this method is very simple and application of the SAXS technique to glass transition problems has been mentioned by several authors[12–14]. It follows from the basic principles of scattering theory, that in a two-phase structure the scattered intensity is proportional to the square of the electron density difference

$$J(\mathbf{b}) \sim (\rho_c - \rho_a)^2 \tag{11}$$

For a temperature range in which no structure changes occur besides thermal expansion, the temperature dependence of the scattered intensity is due to the difference in thermal expansion coefficients of the two phases. Consequently one obtains[13, 15]

$$\{J(T)/J(T)_0\}^{\frac{1}{2}} = 1 + \{(\alpha_a - \alpha_c)/\Delta\rho(T_0)\}\{T - T_0\} \tag{12}$$

where $\alpha_{a,c}$ are the thermal expansion coefficients; for convenience these are defined as change of density per centigrade degree, deviating from a thermodynamic definition. A plot of the square root of relative intensity versus temperature will yield a straight line if the expansion coefficients do not change suddenly. It is noteworthy that the slope of the line does not depend on crystallinity.

A plot of this kind is shown in *Figure 5*, where the square root of the relative intensity is plotted versus temperature for the case of isotactic polybutene-1 crystals grown from solution[13]. Straight lines are observed

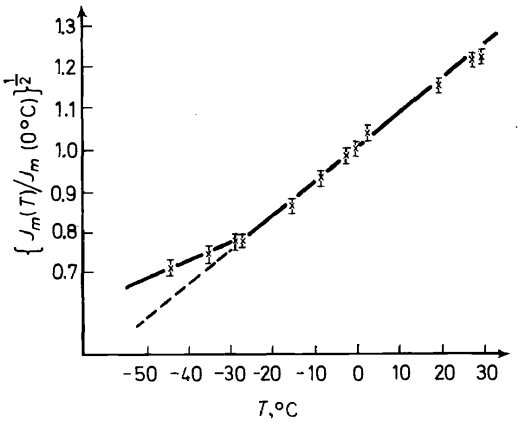

Figure 5. Relative change in peak intensity of the long spacing reflection of polybutene-1 single crystals as a function of temperature[13].

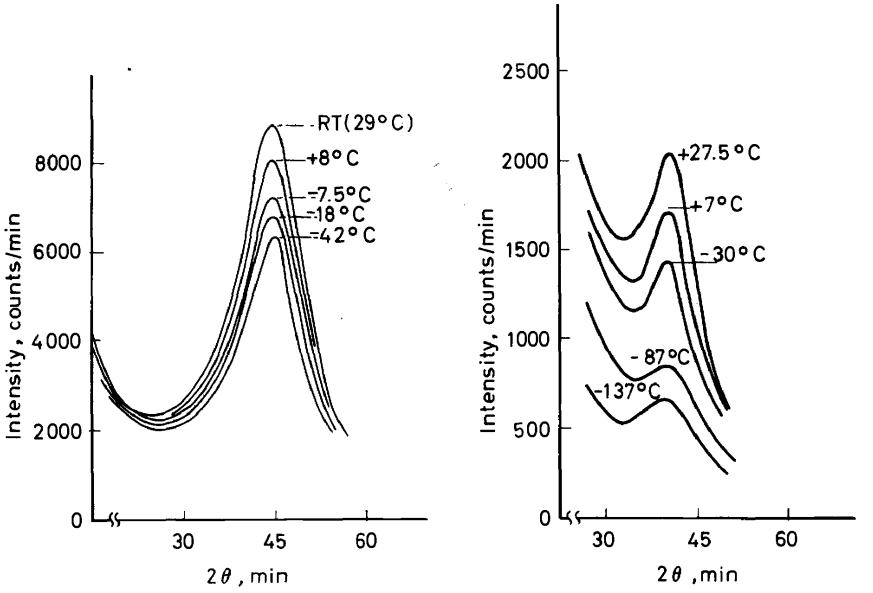

Figure 6. SAXS curves of solution grown polyethylene crystals measured at various temperatures[15]: (a) branched, (b) linear polyethylene.

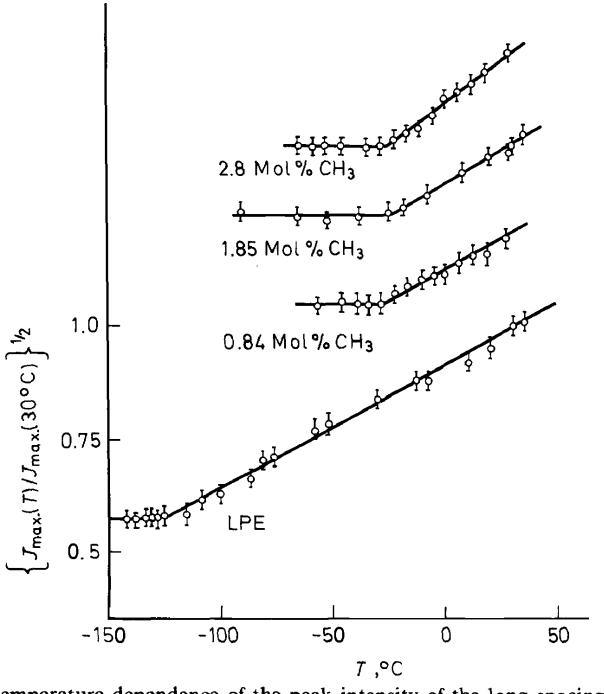

Figure 7. The temperature dependence of the peak intensity of the long spacing reflection of solution crystallized polyethylenes possessing the indicated degrees of CH_3-branching (curves of branched PE are shifted for 0.2 unit along the ordinate).

which exhibit a change of slope in the vicinity of $-25°C$. Evidently at this temperature the expansion coefficient of the disordered phase changes suddenly and the change in slope is an indication of a glass transition at this temperature which is in agreement with the conclusions of other authors.

Similar results are obtained for the case of polyethylene single crystals grown from dilute solution[15]. *Figure 6* shows that in this case too a pronounced temperature dependence is observed; for example, in the case of linear PE the scattering at $-137°C$ is much smaller than that at room temperature. The results of the intensity measurements are plotted in *Figure 7*. There are clear indications of a sudden change in the thermal expansion coefficients of the disordered surfaces of the so-called single crystals, the changes occur at about $-25°C$ for branched polyethylene and at $-125°C \pm 4°C$ for linear polyethylene. In the first case there is no doubt that this temperature is the glass transition temperature of branched polyethylene in accordance with many results obtained from other measurements. The glass temperature of linear polyethylene is a long standing issue of controversy and the temperature of $-125°C$ agrees with the conclusion of other authors[16,17]. For a detailed discussion and further references we refer to our original paper[15].

Besides the usefulness of the SAXS technique for measuring T_g, our results have some significance with regard to the structure of the so-called fold surfaces of single crystals grown from dilute solution. This topic has also been discussed frequently in the past, because of its general importance for all kinds of problems in the field of crystallization of polymers[18]. The existence of some kind of transition in the surfaces of the crystal indicated by the change of expansion coefficient clearly speaks in favour of a structure model characterized by a highly disordered surface, in principle similar to that proposed by Flory[19] in 1962. There are many other problems involved which cannot be discussed in this paper but I hope to have demonstrated the usefulness of SAXS studies for glass transition phenomena.

4. SOLID STATE PHASE TRANSITIONS AND OTHER ANNEALING EFFECTS

It is well known that many polymers show 'polymorphism'. That means they have the property of crystallizing in more than one characteristic structure[20]. During annealing at temperatures well below the melting point a change from one modification to another is very often observed[20], indicating that solid state phase transitions may also occur in macromolecular systems as they are well known both among the chemical elements and the low molecular weight compounds. It is of great interest for the discussion of polymer properties to know more about the molecular mechanism of such solid state transformations, since it may often be hard to visualize the ability of long chain molecules to undergo transition from one kind of crystalline order to another without melting.

With regard to the necessary motion of the molecules in the solid state there is a strong relation between true phase transitions which are reversible with temperature and those structure changes where during annealing an

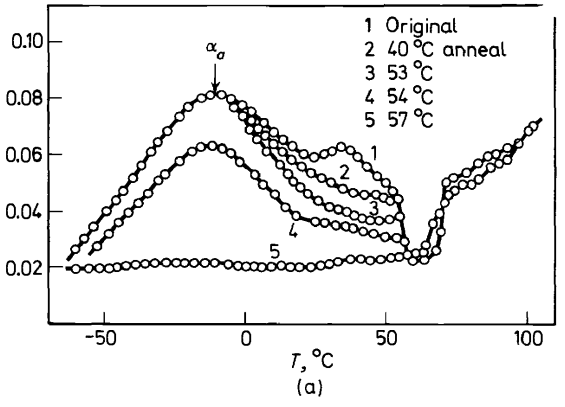

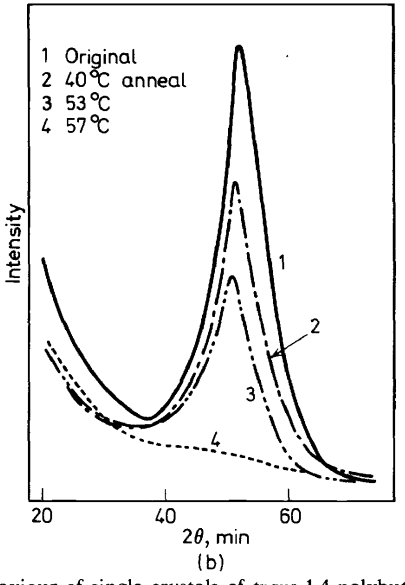

Figure 8. Annealing behaviour of single crystals of *trans*-1,4-polybutadiene (after Takayanagi *et al.*[21]). (a) tan δ curves of single crystals annealed at various temperatures; (b) SAXS curves of single crystals annealed at various temperatures.

unstable structure is transformed into a more stable one. For both kinds of solid state transition one may assume that changes of the morphological structure are also involved.

Whereas many wide angle x-ray diffraction studies on phase transitions have been performed, there are only a few reports on the application of SAXS to these problems. One example is shown in *Figure 8*. Takayanagi *et al.*[21] studied the solid state phase transition of *trans*-1,4-polybutadiene which is known to exist in two crystalline modifications. By annealing at the transition temperature the primary absorption peak of mechanical loss disappears completely, and simultaneously the small angle long spacing

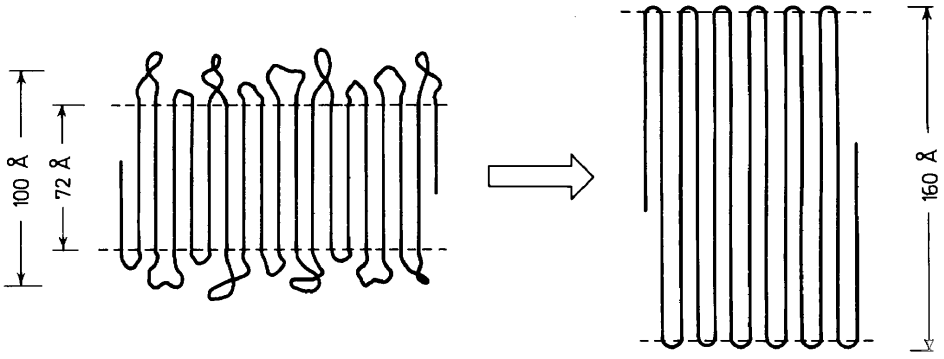

Figure 9. Schematic diagram showing the tightening of loose loops during the solid state transformation of the crystal modification of *trans*-1,4-polybutadiene (after Takayanagi *et al.*[21]).

reflection disappears. The authors concluded from these results that the solid state transition is accompanied by a tightening of loose loops as shown in *Figure 9*. Although this picture may be oversimplified to some extent we may conclude that SAXS yields evidence that the transition of the crystal modification is accompanied by a characteristic change in the structure of the crystal boundaries.

We obtained similar results from small angle studies on the transition of isotactic polybutene-1, which has been reported to occur in the temperature

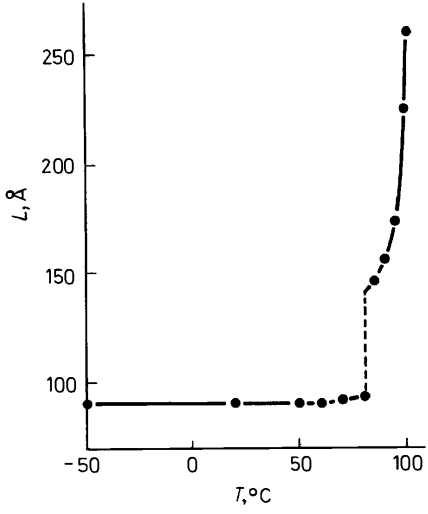

Figure 10. Long spacing of single crystals of isotactic polybutene-1 as a function of temperature[24].

range between 80° and 100°C. The orthorhombic modification transforms to a twinned hexagonal form[20, 22, 23]. This transition is also related to pronounced changes in the morphological structure. The long spacing of

polybutene-1 single crystals increases suddenly at the transition temperature[24], as shown in *Figure 10*. During continued annealing the values of the long spacing remain constant, but the intensity of the reflection increases for a long time, indicating a permanent change in microstructure. From our studies we conclude that this solid state transformation of the crystalline modification cannot be achieved only by the motion of sequences within the crystallites, but the chain units in the amorphous regions are also involved. This example shows that SAXS may be a suitable method for clarifying the molecular mechanism of solid state transitions in polymers.

In this connection it may be mentioned that other kinds of irreversible structure changes taking place during annealing have been observed by SAXS. One example is the well-known 'isothermal thickening', i.e. the increase in thickness of crystals in the chain direction during annealing. This effect, first described by Keller and O'Connor[25] and by Statton and Geil[26], has been studied in many laboratories and different molecular mechanisms have been proposed (for references, see E. W. Fischer[27]). Another effect belonging to this field is the disintegration of defects during annealing which shows up by a change in intensity of the small angle reflections[27]. Although much effort has been spent by many workers in this field, most of the problems related to structure changes in the solid state are still unsolved.

5. PHASE TRANSITIONS AND ORDER–DISORDER PHENOMENA IN *n*-PARAFFINS

Because of the complexity of solid state phase transitions in polymeric systems it may be useful to study phase transition phenomena in oligomeric substances, since one can assume that some characteristic properties for chain molecules will show similar behaviour. Solid state transitions occur in oligomers too, such as the well-known rotational transition in *n*-paraffins. One may hope that understanding of the molecular mechanisms in low molecular weight compounds will help to clarify the nature of the corresponding processes in polymers. Therefore we studied the solid state phase transitions of *n*-tritriacontane $C_{33}H_{68}$ by different methods including SAXS[29, 30].

The study of paraffins is also of interest from the point of view that the temperature dependence of SAXS maxima of paraffins[31, 32] is very similar to that of polymer single crystals[33]. In both cases a strong increase of scattered intensity is observed during heating to temperatures below the melting point. This effect indicates an increase of the density fluctuation in both kinds of samples and can be interpreted generally as an order–disorder phenomenon. Therefore in addition to $C_{33}H_{68}$ a series of long chain *n*-paraffins (C_{60}, C_{62}, C_{70} and C_{94}) has been investigated[29, 30]. Although the studies are not completed up to now we feel that the molecular interpretation of the order–disorder transitions in *n*-paraffins will lead to an understanding of similar processes in polymers, especially of the so-called premelting effects.

The application of SAXS to transition problems in paraffins serves the purpose of characterizing the structure of the interlamellar regions of the paraffin crystals. As an example, *Figure 11* shows the slit-corrected scattering curve of solution crystallized $C_{94}H_{190}$ measured at two temperatures.

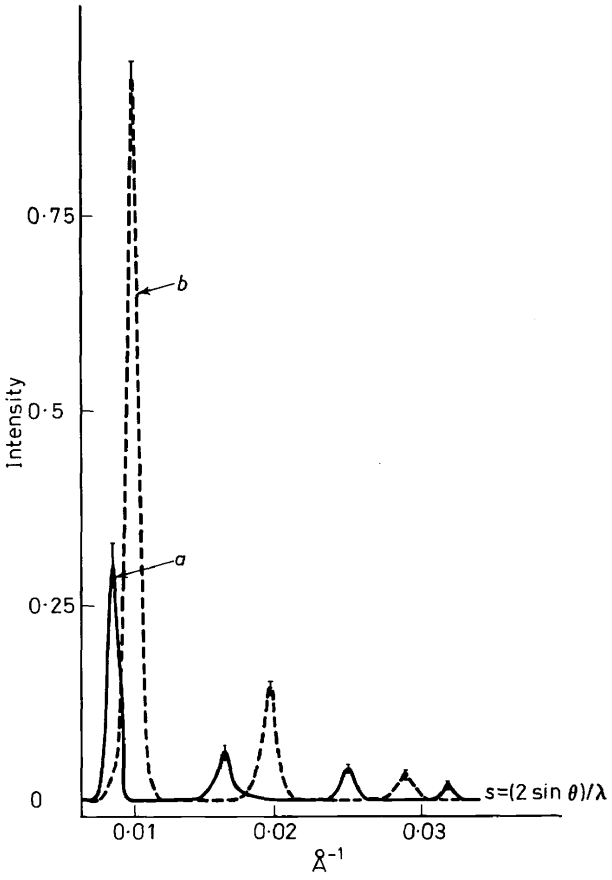

Figure 11. Slit-corrected SAXS curves of solution crystallized $C_{94}H_{190}$ (background scattering subtracted): *a* measured at room temperature; *b* measured at 110°C (according to measurements of G. R. Strobl[29]).

From these curves several quantities can be derived for describing the boundary structure of the paraffin lamellae. The long spacing L follows immediately from the position of the reflections. With regard to their intensities the paraffin molecules can be considered as rods with homogeneous electron density separated by 'holes' between neighbouring rods in the chain direction z. If $\bar{\eta}_p(z)$ is the average electron density distribution of the 'hole' one can define an average scattering power $\langle q \rangle$ measured in electrons per chain

$$\langle q \rangle = \int_{\text{hole}} \bar{\eta}_p(z)\,\mathrm{d}z \tag{13}$$

This quantity yields the number of missing electrons between the lamellae compared with the homogeneous density $\eta = 8/1.27$ electrons/Å of the rods.

A second quantity characterizing the hole structure is the average depth $\langle D \rangle$ of the boundary region[29]

$$\langle D \rangle = (1/\bar{\eta}_{p,\,\max.}) \int \bar{\eta}_p(z)\,\mathrm{d}z \tag{14}$$

In order to evaluate both quantities one may assume an appropriate function $\bar{\eta}_p(z)$ yielding a structure factor $\bar{F}_{00l}$ as a function of the order l which is in agreement with the experimental results. It can be shown[29] that a Boltzmann distribution of the depths of the holes in the lamellae surfaces is a suitable assumption

$$\bar{\eta}_p(z) = \langle q \rangle / \langle D \rangle \exp\{-2|z|/\langle D \rangle\} \tag{15}$$

A straightforward calculation yields[29]

$$\bar{F}_{00l} = \frac{4\langle q \rangle / \langle D \rangle^2}{4/\langle D \rangle^2 + (2\pi l/L)^2} \tag{16}$$

or

$$\frac{1}{\bar{F}_{00l}} = \frac{1}{\langle q \rangle} + \frac{(\pi \langle D \rangle)^2}{\langle q \rangle L^2}\, l^2 \tag{17}$$

A plot of $\bar{F}_{00l}^{-1}$ versus the square of the order l is shown in *Figure 12* for two

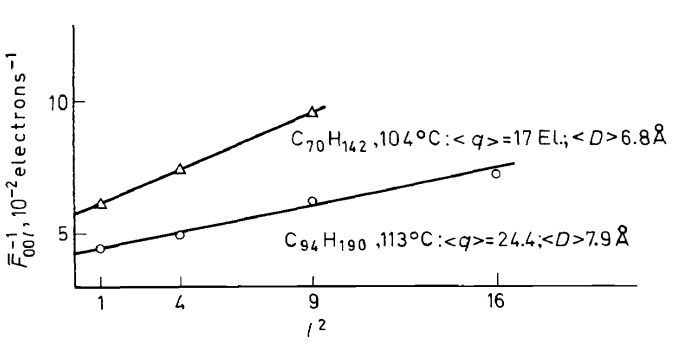

Figure 12. Plot for evaluating the average scattering power $\langle q \rangle$ and the average depth $\langle D \rangle$ of the 'holes' between the paraffin lamellae[29].

examples. In a similar way the dependence of the quantities $\langle q \rangle$ and $\langle D \rangle$ on temperature can be determined for all paraffins under investigation.

During the performance of the small angle x-ray studies of the phase transition in $C_{33}H_{68}$ a rather complex behaviour of this paraffin was observed. Besides the well-known rotational transition at about 66°C two other phase transitions were found as demonstrated in the DSC curve of *Figure 13*. Between room temperature and the melting point at 71°C there exist four crystalline modifications: A, B, C, D. The transitions are accompanied either by changes in the lateral spacings a and b or the thermal expansion coefficients of these spacings[30]. In *Figure 14* the spacings of (110), (200) and (020) lattice planes are plotted versus temperature. At the transition temperature between B and C the (110) and (200) reflections each split up into two separate

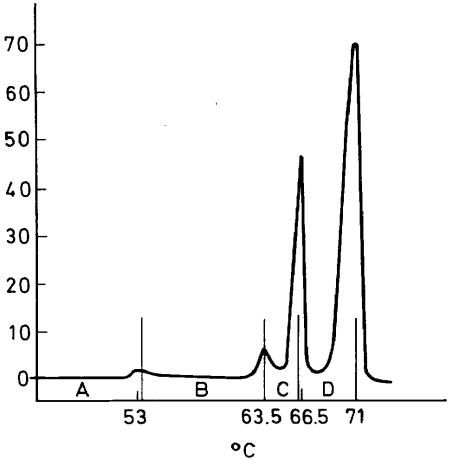

Figure 13. Differential scanning calorimeter curve of a melt crystallized *n*-tritriacontane $C_{33}H_{68}$ showing the existence of four crystalline modifications A, B, C and D (after G. R. Strobl[29]).

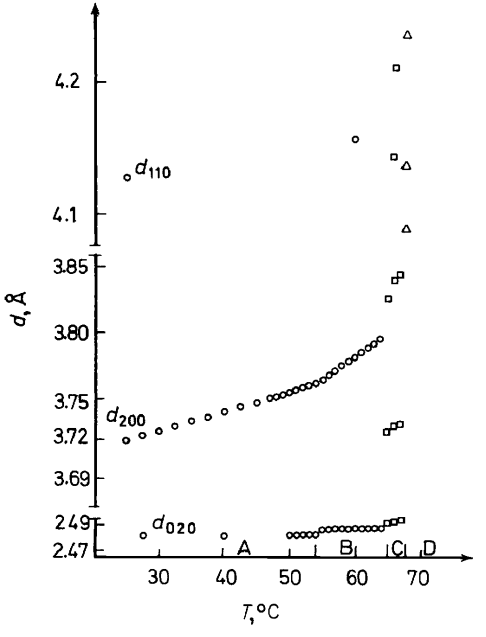

Figure 14. The spacings of (110), (200) and (020) net planes of $C_{33}H_{68}$ as a function of temperature[30] showing the splitting of the reflection at the transitions B → C and C → D. ○ Modification A and B, □ Modification C, △ Modification D ('rotational' phase).

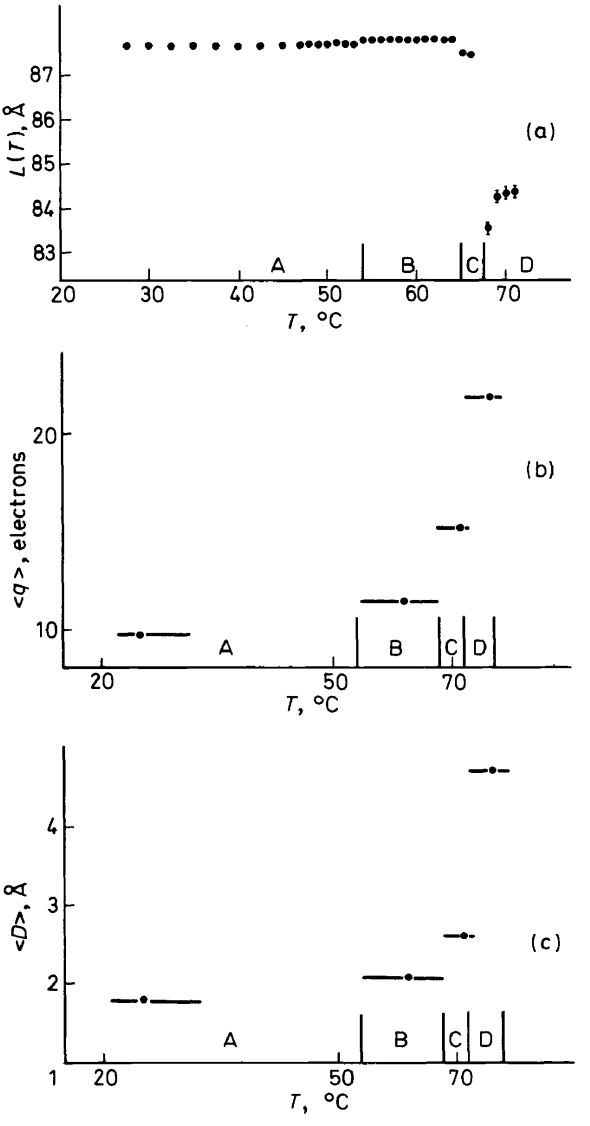

Figure 15. Temperature dependence of the small angle x-ray scattering of melt crystallized $C_{33}H_{68}$: (a) Long spacing L, (b) Average scattering power $\langle q \rangle$ per chain, (c) Average depth of the scattering interlamellar region.

reflections. At higher temperatures the 'rotational' phase D exhibits three different reflections and not only one as one should expect for a hexagonal modification.

The nature of these various phase transitions is not yet known exactly and the subject is still under investigation[30]. With regard to the topic of

our paper we are mainly interested in the behaviour of the long spacing reflections, which is demonstrated in *Figure 15*. There are only small changes in the long spacing L up to the temperature of the so-called rotational transitions (C → D). Above this temperature a sudden decrease occurs which is probably due to a tilting of the chain axis with respect to the normal to the lamellar surface. In addition to the shift of the long spacing reflection a large increase in scattered intensity is observed and accordingly the average scattering power per chain increases from about 10 electrons to 20 electrons. Simultaneously the average depth of the scattering region is increased by almost a factor three*. These results can only be interpreted in terms of an increase in the surface roughness and of 'hole' concentration in the interlamellar region. Therefore the SAXS measurements show that the transition in the lateral packing of the chain molecules in the interior of the paraffin lamellae is accompanied by the creation of disorder in the planes containing the terminal groups of the chains. It will be shown later that with polymers a very similar behaviour is observed.

This result draws attention to a new theory for the rotational transition of the *n*-paraffins proposed by Blasenbrey and Pechhold[34, 35]. They assume that this transition is not due to the rotation of whole chains, but is caused by the creation of special crystal defects, which are called $2g1$-kinks. *Figure 16* shows such a defect originated by the introduction of two *gauche* conformations in a completely stretched chain. The effective chain length is shortened by one CH_2-unit. These authors suggest that the number of kinks increases with temperature as shown schematically in *Figure 17*. Assuming a cooperative interaction of kinks and the creation of larger arrays of kinks (kink-blocks) these authors developed a thermodynamic theory yielding a sharp transition temperature at which the kink concentration changes discontinuously. Because of the shortening of the effective length of the paraffin molecules this transition would lead to an increased roughness of the surface. Therefore our small angle scattering results support this theory, although the problem of the lateral packing of the molecules in the high temperature phase is not quite solved up to now. Further studies of this question are still in progress[30].

Very similar results with regard to the small angle scattering behaviour can be obtained from the long chain *n*-paraffins C_{60}, C_{62}, C_{70} and C_{94} which do not exhibit a so-called rotational transition†. In particular a strong increase of scattered intensity with rising temperature is observed in all cases. Similar results have already been obtained by Sullivan and Weeks[32]. The temperature dependence of the x-ray scattering is demonstrated in *Figure 11* for $C_{94}H_{190}$ as an example. In addition to the intensity changes, a shift of reflection maxima to higher angles, that is a decrease of the long spacing, is found and the intensity ratio of consecutive orders varies with temperature. Qualitatively these scattering curves already show that with increasing

* There is some experimental evidence that the temperature dependence of $\langle q \rangle$ and $\langle D \rangle$ is affected by the crystallization conditions.

† We are obliged to Dr H. D. Keith, Murray Hill, N.J. for supplying the $C_{94}H_{190}$ sample. The synthesis of $C_{60}H_{122}$ and $C_{70}H_{142}$ by Dr W. Heitz and Dipl.-Chem. R. Peters, University of Mainz, is gratefully acknowledged.

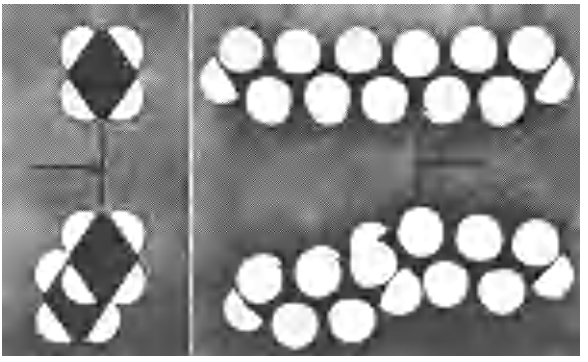

Figure 16. Model of a kink defect. Left hand: planar paraffin chain; right hand: paraffin chain with a $2g1$-kink isomer (after W. Pechhold *et al.*[2]).

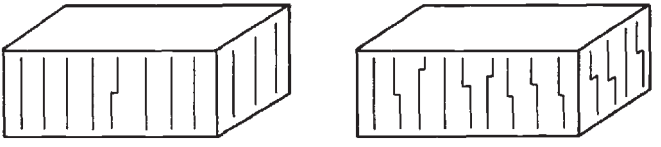

Figure 17. Schematic structure models of a paraffin lamella below and above the transition temperature[35] (the increased roughness of the surface is not taken into account in this drawing).

temperature the surface of the crystals becomes more and more disordered. The observed changes in scattering behaviour must be due to the creation of surface vacancies and an increasing roughness of the crystal surface. As will be shown later, this generally observed feature also applies to the case of polymer crystals in a temperature range where premelting effects are observed macroscopically. This indicates that some type of order–disorder transition also takes place in the surface of polymer crystals.

A more detailed analysis of the scattering curves obtained from *n*-paraffins yields the following results:

The long spacings decrease continuously with increasing temperature during initial heating of solution grown crystals. The relative changes of some samples are plotted in *Figure 18*. During cooling, Lincreases to some extent, but an irreversible behaviour is observed. There exists an obvious difference in the behaviour of solution and melt crystallized paraffins. For a sample of C_{62} crystallized from the melt by quenching a small increase (about three per cent) in long spacing is found during heating, see *Figure 18* d, but the room temperature value of L of this sample is considerably lower (*ca.* 13 per cent) than that of the solution crystallized C_{62}.

The long spacing changes are mainly due to a solid state transformation from the orthorhombic to a monoclinic phase. The transformation is achieved by translating adjacent molecules parallel to the c axis, thus producing a structure in which the plane formed by the terminal methyl groups is tilted

with regard to the chain axis. Therefore the internal structure in both phases is the same, differences only arise in the packing of the end groups. Thermodynamically the monoclinic structure is the more stable form for even alkanes[36–38]. In accordance with the x-ray results the electron microscopical

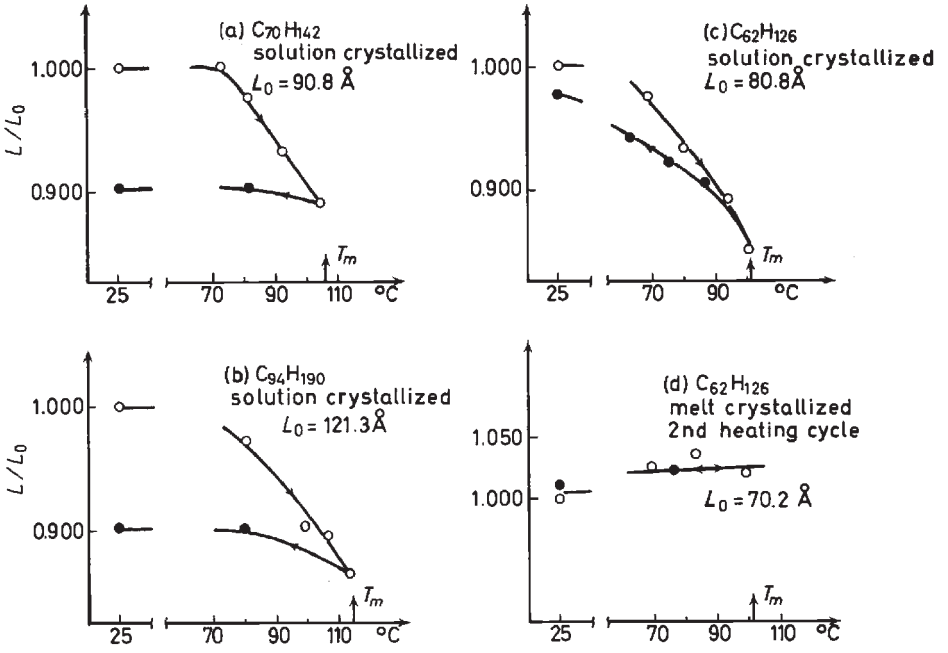

Figure 18. The relative changes in long spacings of *n*-paraffin crystals depending on temperature (according to measurements by G. R. Strobl[29]): ○ heating ● cooling.

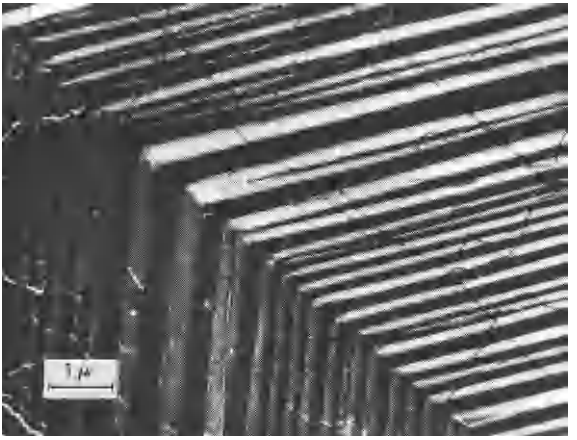

Figure 19. Surface replica of a $C_{94}H_{190}$ crystal after heating to 110°C (electron micrograph by I. G. Voigt-Martin[30]).

studies reveal the development of ridges in paraffin crystals which are essentially flat at room temperature. As an example *Figure 19* shows the structure of a C_{94} crystal after heating to 110°C. The ridges run parallel to the direction of the (200) lattice planes, indicating that the translation of molecules in the *c* direction took place between neighbouring molecules along the *a* axis of the paraffin crystals. This result will be of some relevance for the later discussion of the structure of the paraffin crystal surface. The same effect has been observed by Keller[39] after heating $C_{36}H_{74}$ crystals to temperatures above 65°C.

The development of ridges and the accompanying changes in the coarse texture of the paraffin crystals is an irreversible process yielding a more or less irreversible change in the long spacing (*Figure 18*). The original reason is the increasing space requirement of the terminal methyl groups. The demand for more free volume per CH_3 unit can be satisfied by developing structures characterized by staggering the chain molecules in the *c* direction. It is noteworthy that a similar effect has been observed with polyethylene single crystals by Keller and co-workers[40]. Polyethylene crystals grown at 90°C showed a decrease in long spacing when annealed between 95°C and 125°C; this has been explained in terms of the rearrangement of fold packing.

Besides the changes of long spacing the temperature dependence of the scattered intensity is of special interest for discussing the order–disorder transitions in *n*-paraffins. Generally one would expect the intensity of the reflection maxima to decrease with increasing temperature. The strong increase in intensity of the 00*l* reflection at temperatures near the melting point will yield valuable information about the disorder phenomena or premelting effects in long chain paraffins.

The intensity changes can be described by evaluating the average scattering power $\langle q \rangle$ per chain molecule normalized to the scattering power of one electron. This quantity can be calculated according to equation 17 from the absolute values of the scattered intensities. The temperature dependence of the scattering power of some samples is plotted in *Figure 20*. An increase of $\langle q \rangle$ for a factor up to 2.5 is observed, this being equivalent to an increase of scattered intensity of about six times.

In the case of solution crystallized samples, all paraffins under investigation showed a scattering power of about ten electrons per chain at room temperature, corresponding to a 'hole' between subsequent lamellae with a length $a = 1.95$ Å. This is in perfect agreement with the difference between the long spacing L and the length of the molecule

$$a = L - 1.25\,n[\text{Å}]$$

The change of scattering power is not quite reversible. For example, with C_{94} a value of $\langle q \rangle = 15$ electrons is observed at room temperature after running the sample through a heating cycle. This value is equivalent to a hole having an average length $\langle D \rangle = 2.7$ Å and can be explained easily by the partial solid state transformation to a staggered structure. Its occurrence had already been concluded from the changes in long spacing. According to the x-ray data for paraffins with monoclinic structure, the staggered phase is accompanied by a 'hole' of 2.93 Å between adjacent lamellae[36].

In addition to the increased scattering due to the staggering of chains, a

strong increase in $\langle q \rangle$ is observed which clearly indicates a temperature-dependent disorder in the CH_3 terminal planes of the paraffin crystals. The higher the temperature the larger is the 'roughness' and the number of defects within that plane. According to our preliminary results the amount of disorder seems to depend reversibly on temperature, but it is affected remarkably by the crystallization conditions. For example, melt crystallized C_{62} already starts with a scattering power of 25 electrons at room temperature, see *Figure 20*. At 101°C this quantity amounts to almost 50 electrons, corresponding to surface voids having an average length of 8 Å, whereas the long spacing

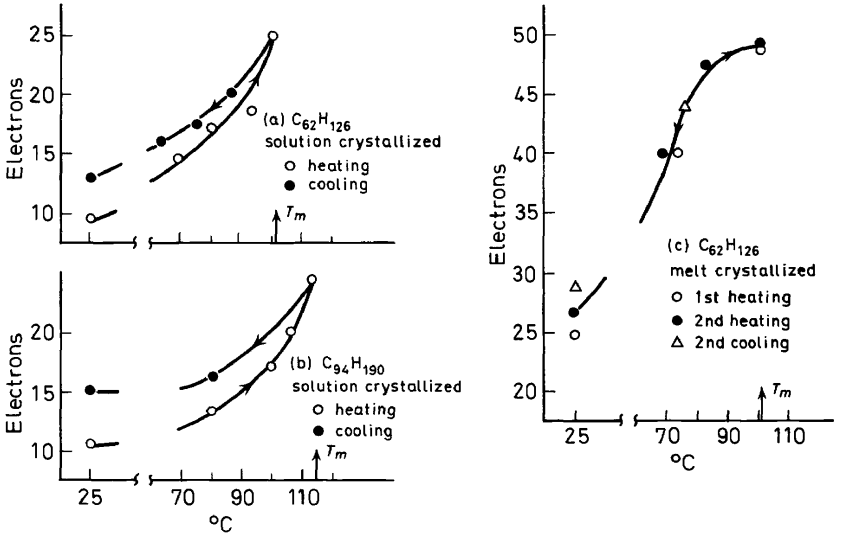

Figure 20. Dependence of the average scattering power $\langle q \rangle$ of *n*-paraffin samples on temperature during heating and cooling cycles (after measurements by G. R. Strobl[29]).

changes are only in the range of 2.0 Å, see *Figure 18*. Evidently the amount of disorder introduced during heating depends on the number of defects originally existing.

The values of the average depth $\langle D \rangle$ of the scattering surface region and the fluctuation δ of the lamellar thickness have also been evaluated from the scattering data. In accordance with the intensity increase, $\langle D \rangle$ increases with rising temperature. For example, with C_{94} the depth $\langle D \rangle$ changes from 2 Å at room temperature to 7.6 Å at 113°C. With regard to the effect of crystallization conditions values of $\langle D \rangle$ equal to 2.0 Å and 4.8 Å were found for C_{62} crystallized from solution and the melt respectively[29].

The fluctuation δ in the regularity of the crystal in the c direction which can be calculated from the linewidth of reflections of different order l is approximately equal to[29]

$$\delta = \overline{(\delta \hat{L}/\hat{L})} + \overline{3(\pi \delta L/\hat{L})^2}$$

where $\delta \hat{L}$ is the fluctuation in the average long spacing $\hat{L}$ of the crystals and

δL is the fluctuation in the long spacings L within one crystal with the average long spacing $\bar{L}$. In most solution crystallized samples δ was found to be zero at room temperature, indicating almost perfect crystals*. With rising temperature δ increases to values of two to six per cent; at still higher temperatures a slow decrease is observed. This distortion of the lattice is probably due to the non-uniform transformation from the orthorhombic to the staggered crystal modification, which also explains the observation of a continuous change in the long spacings, see *Figure 18*.

Summarizing the results of the small angle x-ray studies of *n*-paraffins one may conclude that the oligomeric crystals undergo a pronounced order–disorder transition with respect to the structure of the lamellar boundaries containing the terminal groups of the chains. This process already starts far below the melting point, it increases continuously with rising temperature and produces a maximum of disorder just at T_m. One may call this phenomenon and the accompanying disruption of the planar arrays of the terminal groups a '*surface premelting of chain molecular crystals*'. A very similar effect is also observed with polymer crystals, as we will show later.

The molecular nature of the 'surface premelting' of *n*-paraffins can be visualized on the basis of our knowledge about the kinds of characteristic defects of crystals consisting of chain molecules. In *Figure 22* a very speculative and schematic drawing of the structure of a paraffin crystal is represented,

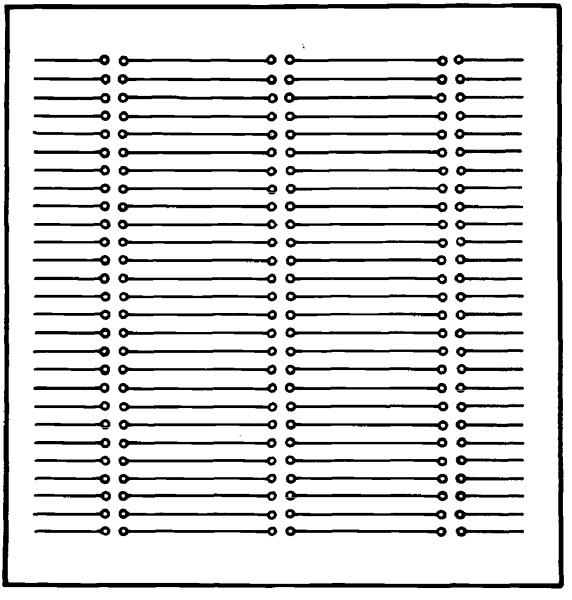

Figure 21. Schematic drawing of the structure of a long chain paraffin crystal at room temperature (orthorhombic modification).

* From the line width of the 00*l* reflections the sizes of the coherent crystal regions could be estimated to amount to about 10 to 20 lamellae per crystal depending on crystallization conditions.

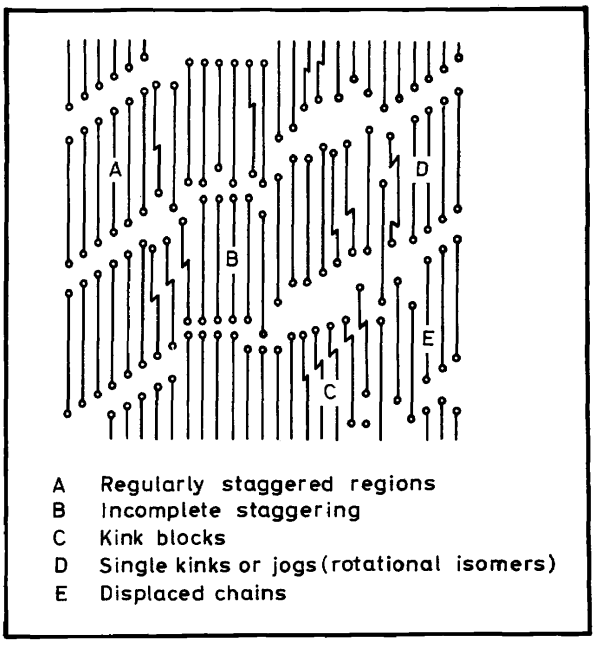

Figure 22. Schematic drawing of the structure of a long chain paraffin crystal at a temperature some degrees below the melting point.

which it is proposed emerges from the regularly ordered form of *Figure 21* by heating to temperatures near the melting point. Besides regions consisting of regularly staggered molecules, various types of disorder exist in the crystal at higher temperature: (i) regions with incomplete or no staggering of the molecules, (ii) surface vacancies created by kink-blocks, i.e. cooperatively interacting arrays of special rotational isomers[34, 35], (iii) point vacancies due to single kinks or jogs or so-called Reneker defects and finally (iv) row vacancies caused by larger displacements of chains along the axis. All these defects give rise to the roughness of the lamellar boundaries; some have already been discussed recently by Sullivan and Weeks[32].

The amount and the extension of disorder can be measured quantitatively by the quantities $\langle q \rangle$, $\langle D \rangle$ and δ evaluated from the intensities and shape of the (00*l*) reflections. Evidently macroscopic voids caused by collapse difficulties[32] cannot be regarded as the origin of the observed effects, since they will only yield an additional background scattering.

The real structure of the disordered interlamellar regions is determined by the intermolecular forces and because of the high mobility of the chains a structure will develop which is characterized by the lack of crystalline order and by a thermodynamically determined 'free volume'. One may or may not call the interlamellar region an 'amorphous' surface layer; this seems to be more a semantic than a physical problem.

The subject of 'homophase premelting', as defined by Ubbelohde[1], has been discussed extensively in the past. Experimental evidence for premelting

of *n*-paraffins has been published, most recently by Atkinson and Richardson[38]. One of the main experimental difficulties in tackling this problem is the fact that the macroscopically measured thermodynamic quantities do not enable a differentiation to be made between this phenomenon and a 'hetero-phase premelting', for example due to a freezing point depression spread caused by impurities. The SAXS technique, however, can localize the spot of phase transition and it can yield valuable additional information. With regard to the theoretical explanation for partial melting of molecular crystals of chain molecules the first step was taken by Flory and co-workers[41]. Along this line the theoretical problem of premelting can be solved by taking into account the thermodynamic properties of the various defects outlined in *Figure 22*.

6. PARTIAL MELTING AND PREMELTING EFFECTS IN HIGH POLYMERS

The most important phase transition in the polymer field is the melting of partially crystalline polymers. It is not only of great scientific interest but also of great importance in the processing and performance of polymers for all technological applications. The change in properties of plastics, fibres and elastomers with temperature depends largely on both the melting point and on certain premelting effects, which we will now consider in more detail.

It is known that polymers generally exhibit the phenomenon of partial melting, that means the degree of crystallinity decreases continuously with temperature within the so-called melting range. The behaviour can be studied most easily by measuring the heat capacity or the specific volume of the sample. The temperature of melting as well as the extension of the melting range depend on the crystallization conditions, on the molecular weight distribution and on the chemical homogeneity of the macromolecules. As an example for the influence of crystallization temperature *Figure 23* shows the temperature dependence of the specific volume of natural rubber crystallized at various temperatures. These measurements were made by Wood and Bekkedahl[42] as early as 1946. The influence of modifying the chemical structure of the molecules is demonstrated in *Figure 24*, where the temperature dependence of the specific volume of trioxan–dioxolane copolymers is plotted for various concentrations of co-units[43]. It was attempted to achieve as high a crystallinity as possible by annealing. The melting point depression and the broadening of the melting range are well known features in the melting behaviour of copolymeric systems and have been observed for a large number of polymers. We chose the example of *Figure 24* because some of the SAXS experiments described later have been performed on this system.

If the temperature dependence of the unit cell dimensions of the crystalline regions is known from x-ray wide angle experiments, the degree of crystallinity can be calculated from the specific volume by a simple equation, provided that three essential assumptions are introduced: (i) that the specific volume is simply additive, that means that the properties of each phase are independent of the amount of the other phase, (ii) that the crystalline phase has the structure of a perfect crystal and (iii) that the amorphous phase has the specific volume of the melt extrapolated to low temperatures. Using these assumptions

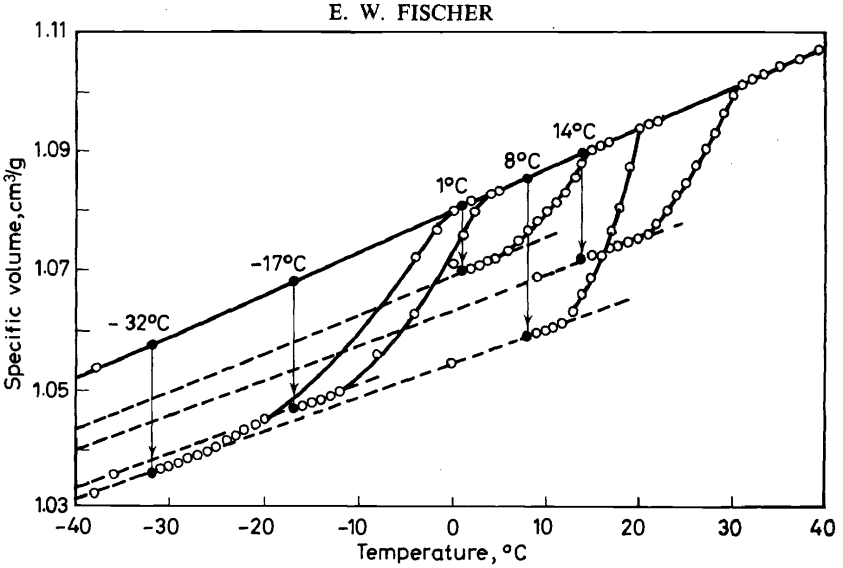

Figure 23. Melting curves of natural rubber as a function of crystallization temperature (after L. A. Wood and N. Bekkedahl[42]).

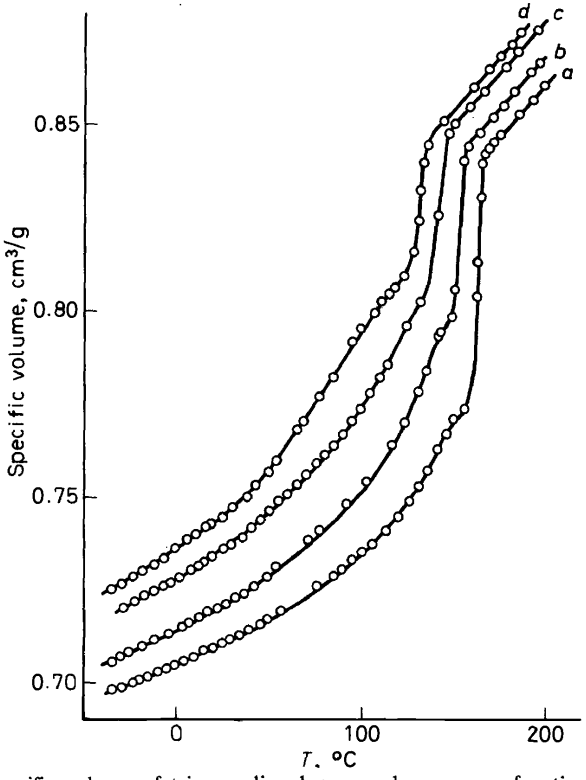

Figure 24. Specific volume of trioxan–dioxolane copolymers as a function of temperature (according to measurements by H. Wilski[43]): (a) 2.7 Mol% dioxolane, annealed at 150°C, (b) 5.9 Mol% dioxolane, annealed at 147°C, (c) 11.0 Mol% dioxolane, annealed at 134°C, (d) 17·4 Mol% dioxolane, annealed at 121°C.

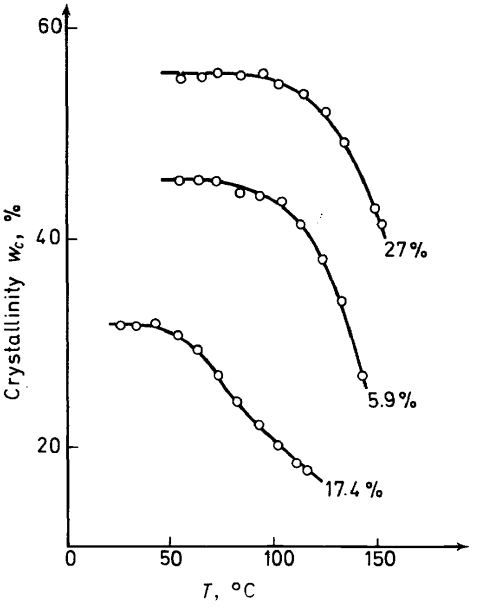

Figure 25. Variation of the degree of crystallinity of trioxan–dioxolane copolymers with temperature[44].

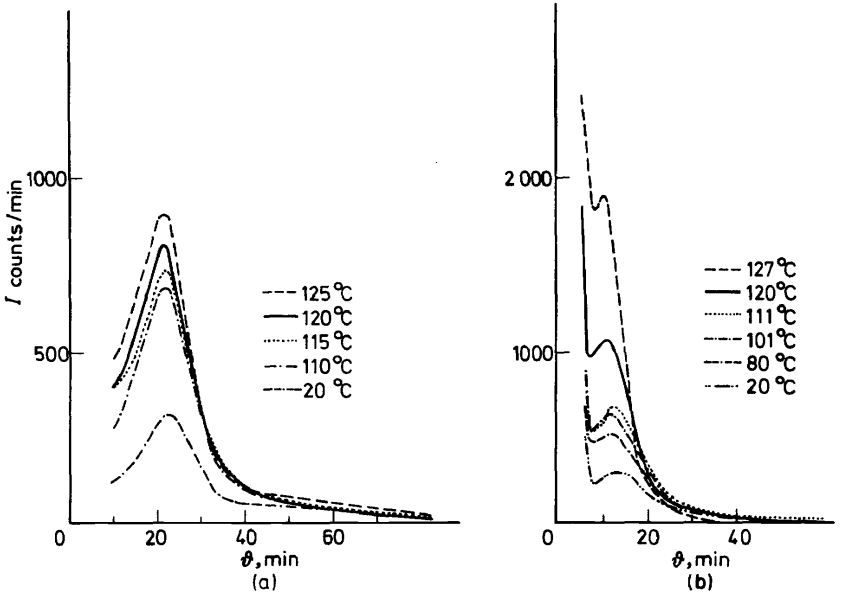

Figure 26. SAXS curves of polyethylene single crystals measured at various temperatures[56]. The samples were annealed before measuring at (a) 125°C, (b) 130°C.

a temperature dependence for the degree of crystallinity is obtained as shown in *Figure 25*, where the dependence of the size of the unit cell on the copolymer concentration has been taken into account[44]. One of the most important applications of SAXS to melting problems is in fact the verification of these three assumptions, as we will show later. Without experimental proof by small angle scattering, the calculation of crystallinity from macroscopic data is less certain[28, 45].

Various theories have been proposed for the explanation of the partial melting of polymers, starting with the famous work of Flory[46] in 1949. For the theoretical interpretation of the observed behaviour some basic assumptions must be introduced regarding changes in the texture of the partially crystalline sample which take place during the melting process. We do not want to review the various theories and proposals, but the aim of the following section is rather the derivation of suitable structure models in order to explain the scattering behaviour and its dependence on temperature.

In this respect one of the most important features of SAXS studies is the tremendous increase in scattered intensity with increasing temperature. *Figure 26* shows scattering curves of polyethylene single crystals measured at various temperatures. As we pointed out several years ago the observed increase cannot be explained by thermal expansion[33, 27], since the difference in the thermal expansion coefficients would only lead to a much smaller increase in the scattering power. In addition the intensity changes can be quenched, i.e. rapid cooling yields samples with higher scattering power than does slow cooling. This result suggests a correlation between changes of scattering pattern and partial melting. It also shows a similarity to the premelting effects observed with long chain paraffins.

The described intensity changes are rather generally observed when

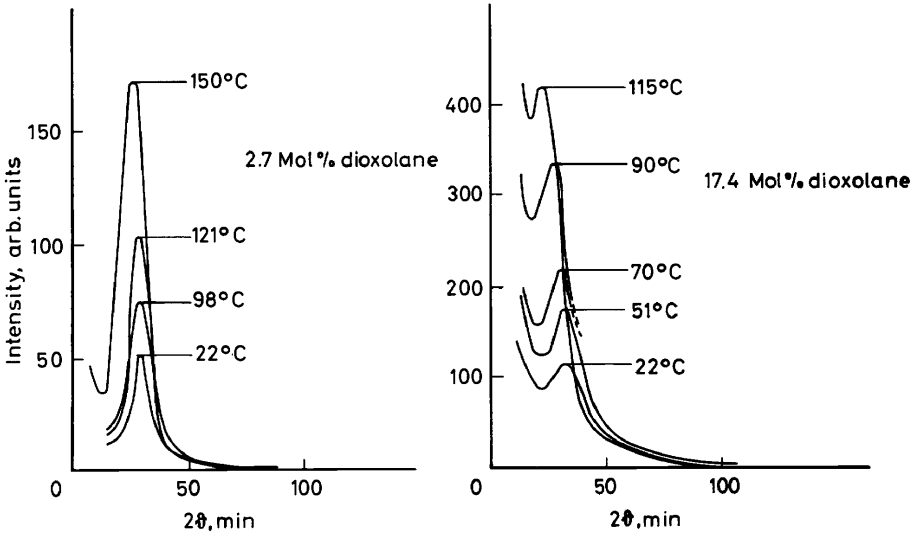

Figure 27. Slit-corrected SAXS curves of trioxan–dioxolane copolymers measured at the indicated temperatures[44].

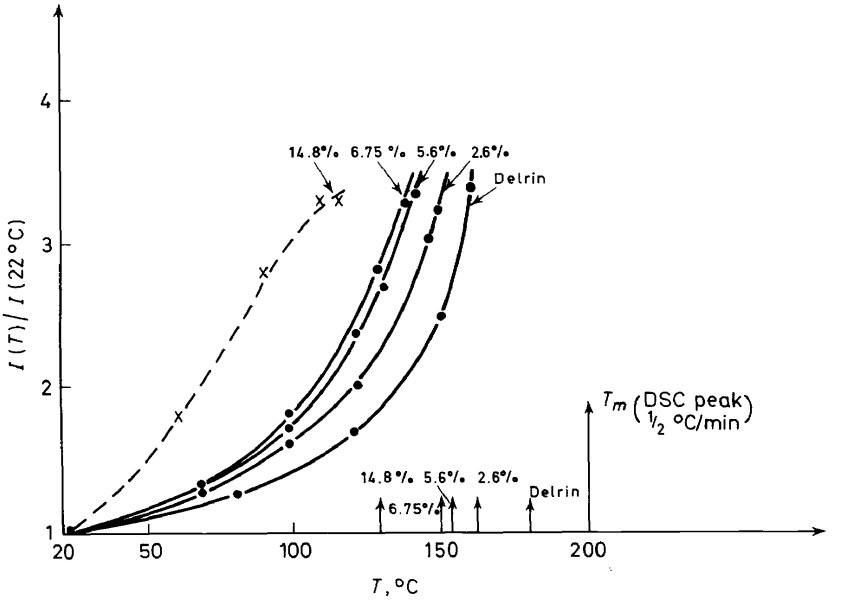

Figure 28. Variation of the relative peak intensity of the small angle reflection with temperature[44]. The arrows indicate the DSC-melting points of the various trioxan–dioxolane copolymers.

studying crystalline polymers. It has been found with polyethylene crystallized from the melt[47], drawn polyethylene[48], branched PE[49], POM both oriented and un-oriented[50], polypropylene[51], 6-nylon[52], and other polymers. As an example *Figure 27* shows the SAXS curves of trioxan–dioxolane copolymers measured at various temperatures[44]. Here also a strong increase in scattered intensity is observed. Within the indicated range of temperatures the scattering behaviour is completely reversible with temperature; irreversible changes are only observed if the original annealing temperatures of the samples are exceeded.

As with polyethylene single crystals mentioned above, it can be shown that the strong increase in intensity is not only due to thermal expansion effects, but it is caused by the partial melting of the copolymers (see *Figure 25*). The relationship between intensity increase and melting can be demonstrated by *Figure 28*, where the relative intensity changes are plotted versus temperature[44]. The curves are shifted to lower temperatures for copolymers with a lower melting point. Obviously thermal expansion effects should not depend on melting point. For the same reason the possibility of standing thermal waves as origin of the long spacing reflections[53] can be excluded.

A quantitative proof of this relationship can be achieved by comparing the small angle x-ray results with the specific volume measurement. The scattering power of the copolymer samples was measured according to equation 9 as a function of temperature. The mean square density fluctuation derived from these measurements can be compared with the values calculated from the specific volume assuming a two-phase structure. *Table 1* shows that a

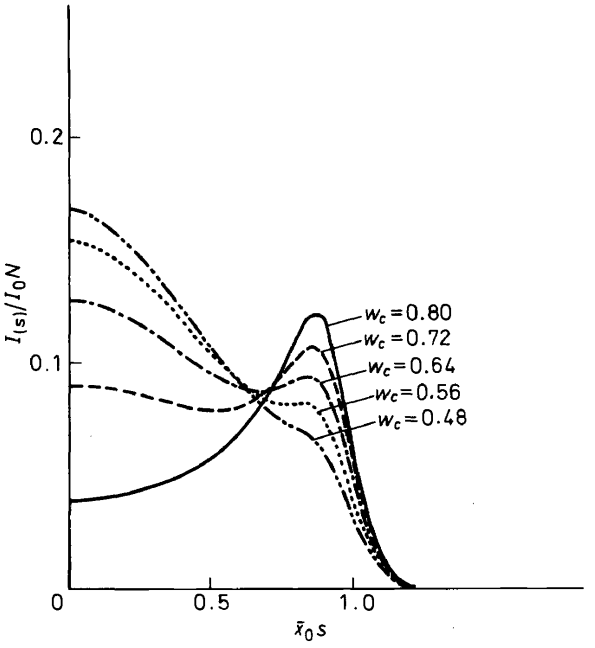

Figure 29. Dependence of calculated scattering curves on degree of crystallinity w_c. The curves were calculated using the assumption that some statistically distributed crystallites melt completely[54].

Table 1. Comparison of measured and calculated scattering powers of trioxan–dioxolane copolymers

Mol% dioxolane	*Temp.* °C	*Measured* $\langle\eta^2\rangle \times 10^{-3}$ [Mol electrons/cm^3]	*Calculated* $\langle\eta^2\rangle \times 10^{-3}$ [Mol electrons/cm^3]	$(\langle\eta^2\rangle/\langle\eta^2\rangle^*)^{\frac{1}{2}}$
2.7	22	8.1	7.8	1.02
	68	9.5	9.8	0.98
	98	12.5	11.3	1.05
	121	13.6	12.5	1.04
	146	15.6	13.4	1.08
	150	15.7	13.6	1.07
5.9	22	9.1	8.5	1.03
	68	11.7	10.9	1.03
	98	13.5	12.3	1.05
	121	14.8	12.8	1.08
	130	14.6	12.7	1.07
	141	13.9	11.6	1.09
17.4	22	7.9	7.5	1.02
	51	9.3	8.9	1.02
	70	9.6	9.0	1.03
	90	8.1	8.7	0.97
	109	8.8	8.4	1.02
	115	8.7	8.3	1.02

reasonable agreement between both values is obtained. Consequently the ratio of the measured to the calculated density fluctuation is almost equal to one over the whole range of temperatures. Hence the copolymer can be considered as being composed of crystalline regions corresponding to the x-ray crystalline density and amorphous regions with the density of the supercooled melt. These results prove: (i) that the assumptions of a two-phase model are correct and (ii) that the intensity changes are due to partial melting besides the influence of thermal expansion. It may be mentioned that with regard to the verification of the two-phase model in the case of other copolymers different results can be obtained[45].

So far we have proved that the increase of the overall scattered intensity or of the scattering power is due to the partial melting of the polymer sample.

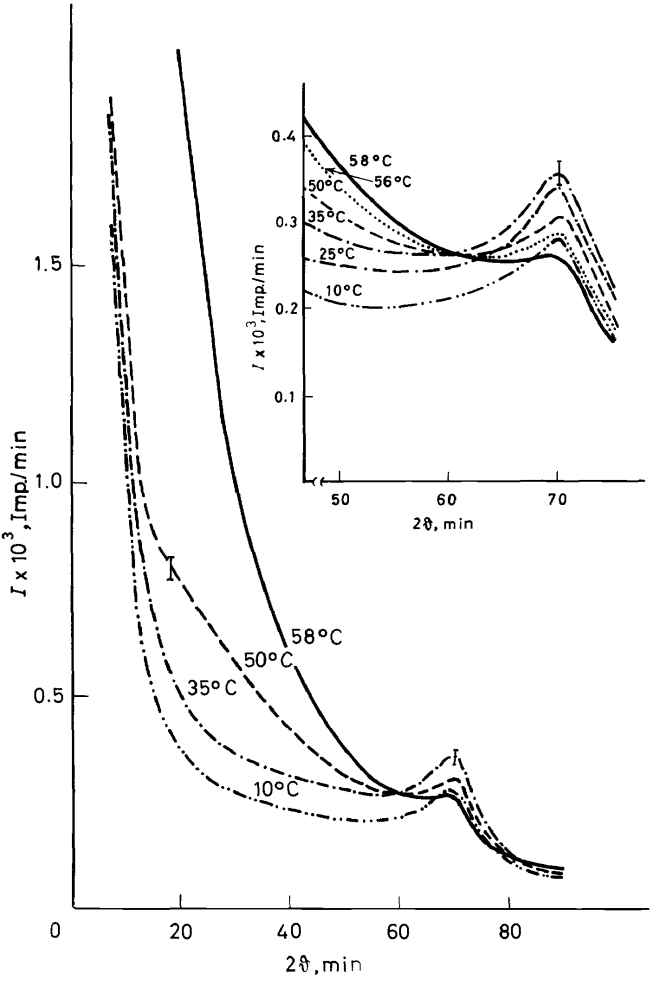

Figure 30. SAXS curves of polyethylene oxide single crystals measured at the indicated temperatures[55].

Now the important question arises: What kind of structure changes take place during melting? In other words, one has to solve the problem of how the temperature dependence of the shape of the scattering curve can be explained. Obviously the answer to this question will yield important information about the mechanism of partial melting in polymer systems.

A very commonly accepted model of the partial melting process assumes that the spread of fusion over a large temperature range is due to a distribution of crystallite sizes and perfection. Since both quantities affect the melting

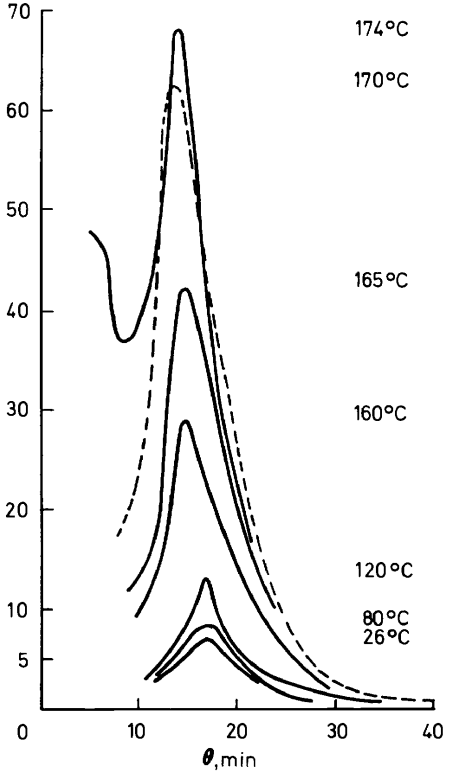

Figure 31. Slit corrected SAXS curves of polyoxymethylene (Delrin) measured at the indicated temperatures[57].

point of a crystal there is no doubt that such influences may occur. One can calculate the dependence of scattering curves on crystallinity for such a model using, for example, a paracrystalline superlattice with decreasing number of scattering elements. The result is shown in *Figure 29*[54]. These curves have been calculated on the basis of the assumption that within a one-dimensional infinitely large stack of crystallites some statistically distributed crystallites melt. The integrated intensity increases due to melting, the peak intensity of the reflection decreases drastically, however. This result can be imagined rather easily without calculation, since the melting of some crystallites

causes a large increase in the statistical fluctuation of the distances between the remaining scattering units. Therefore the scattering background will increase at the cost of the peak intensity.

Obviously the theoretically derived prediction based on this model is in contrast to the observed behaviour of the majority of polymers which we described above, see *Figures 26* and *27*. In these cases a strong increase of reflection intensity with decreasing crystallinity was observed. Nevertheless we actually found one case showing the predicted intensity changes. In *Figure 30* scattering curves of unannealed PEO single crystals are plotted[55]. With increasing temperature the background intensity increases and the reflection intensity decreases. The reason for the deviating behaviour of polyethylene oxide single crystals is not yet known. *Figure 30* demonstrates, however, that some polymeric structures may exist where the partial melting is due to fusion of whole crystallites.

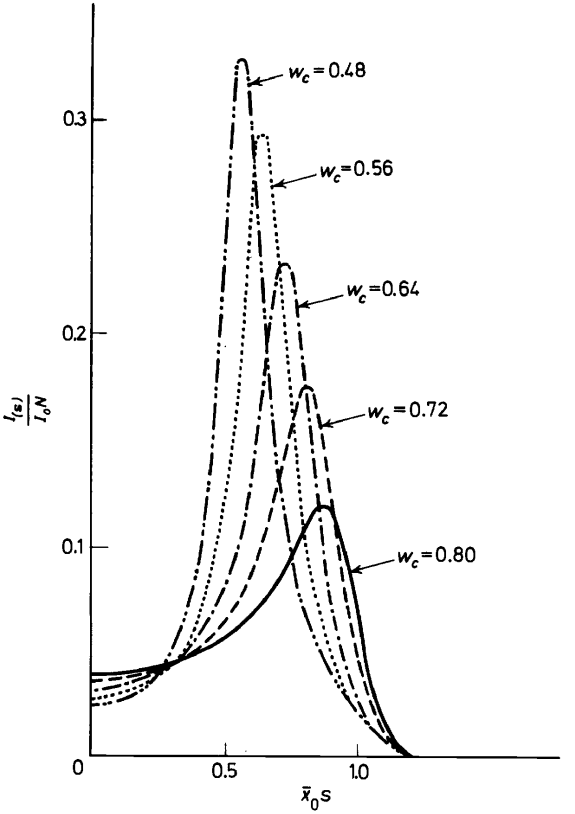

Figure 32. Dependence of calculated scattering curves on degree of crystallinity w_c. The curves were calculated assuming that the decrease in crystallinity is due to an increase in thickness of the amorphous intercrystalline layers[54].

Going back to the 'normal' behaviour *Figure 31* shows again the large increase in reflection intensity at higher temperature[57], in contrast to the calculated scattering curves of *Figure 29*. Obviously this behaviour cannot be explained by a model assuming melting of whole crystallites. Now we shall treat another model assuming that the thickness of the intercrystalline layers increases continuously with temperature. In this case a scattering behaviour as shown in *Figure 32* is calculated in qualitative agreement with the observed behaviour. In analogy to the definition of 'surface premelting' of molecular crystals which we introduced for the description of the results of our paraffin studies, we describe the similar effect in polymers as '*boundary premelting*'.

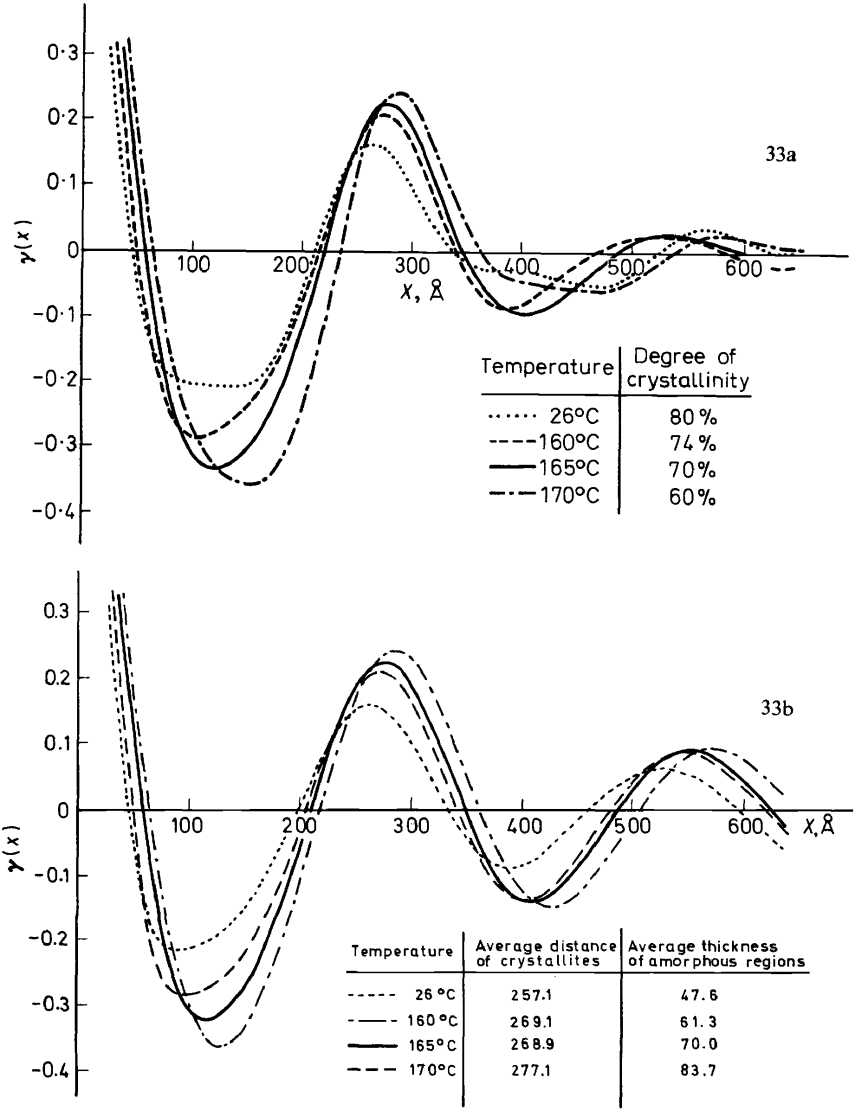

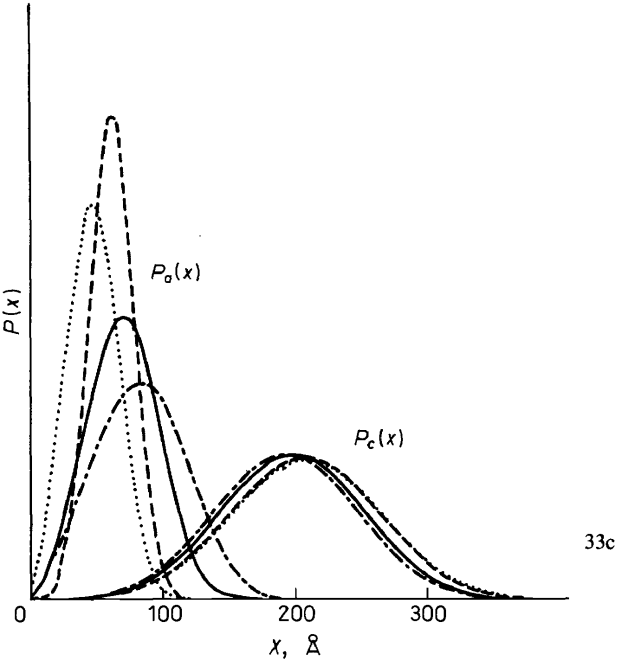

Figure 33. Example for analysing the scattering behaviour by means of comparing measured and calculated values of the correlation function $\gamma(x)$[57]. (a) Correlation functions obtained from the scattering curves of polyoxymethylene measured at the indicated temperatures. (b) Calculated correlation functions of a model consisting of lamellae with thickness distribution $P_c(x)$ and intercrystalline layers with thickness $P_a(x)$. The model parameters were selected for fitting to the measured curves of *Figure 33*(a). (c) Distribution functions $P_c(x)$ and $P_a(x)$ of the thicknesses of the crystals and amorphous regions.

Although qualitative agreement between the observed and the calculated scattering pattern can be established on the basis of the 'boundary premelting' model, the very difficult task of a quantitative interpretation of the scattering behaviour is not yet completed. A better approach for solving this problem is the comparison between measured and calculated correlation functions $\gamma(x)$. One advantage of this method is the elimination of density effects since the correlation function is normalized by the scattering power according to equation 4. The correlation functions can be calculated for different melting models using the procedure proposed by Vonk and Kortleve[58].

Figures 33 (a), (b) and (c) show some preliminary results of the application of this analysis to the melting of polyoxymethylene[57]. In *Figure 33* (a) the correlation functions $\gamma(x)$ calculated from the scattering curves are plotted. The scattering curves were measured at the indicated temperatures, the corresponding degrees of crystallinity were obtained from the scattering power of the samples. In order to analyse the dependence of changes in structure on temperature, correlation functions $\gamma(x)$ were calculated for a model consisting of lamellae with a thickness distribution $P_c(x)$ and intercrystalline amorphous layer with a thickness distribution $P_a(x)$. Calculated

functions are shown in *Figure 33* (b), the corresponding distribution functions are plotted in *Figure 33* (c). The parameters of the distribution functions were varied until the best fit between calculated and measured correlation functions was obtained with regard to (i) the first intersection of $\gamma(x)$ with the abcissa, (ii) the depth of the first minimum and (iii) the height and position of the first maximum. The distribution functions of *Figure 33* (c) show that with increasing temperature there is a small decrease in the average crystal thickness and a large increase in the average thickness of the intercrystalline layers. We consider this result again as being proof of the proposed boundary premelting process.

The results of the SAXS experiments show that in many cases partial melting of polymers is due to the creation of additional disorder at the surface of the crystallites. As already pointed out this phenomenon is very similar to the surface premelting of paraffin crystals. The intensity variations as a function of temperature are reversible under suitable conditions; therefore the premelting effects can be treated by a theory based on the assumption of a hindered thermodynamic equilibrium. Qualitatively one can realize easily that the increase in entropy due to the additional disorder at the surface minimizes the free energy of the whole system. Therefore it has been proposed that the thickness of the disordered surface layer is governed by an *equilibrium length* $N_{eq.}$ of the non-crystallized sequences[33, 59, 60]. For a quantitative calculation of $N_{eq.}$ certain statistical models have to be introduced in order to calculate the entropy of the amorphous layers. Several fruitful attempts have been made to this end, especially by Zachmann and co-workers[61]. For detailed information we refer to recent review articles by Zachmann[62] and by Fischer[27].

ACKNOWLEDGEMENTS

This work was carried out as a project of the 'Sonderforschungsbereich 41 der Deutschen Forschungsgemeinschaft'. I gratefully acknowledge the financial support by the DFG. I also thank Dr I. Voigt-Martin for her help in preparing the manuscript of this paper.

REFERENCES

[1] A. R. Ubbelohde, *Melting and Crystal Structure*, Clarendon Press: Oxford (1965).
[2] W. Pechhold and S. Blasenbrey, *Kolloid-Z.u.Z.f.Polym.* **216/217**, 235 (1967).
[3] W. Pechhold, *Kolloid-Z.u.Z.f.Polym.* **228**, 1 (1968).
[4] O. Kratky, *Z. Elektrochemie*, **58**, 49 (1954).
O. Kratky and A. Sekora, *Mh. Chem.* **85**, 660 (1954).
[5] E. W. Fischer, H. Goddar and G. F. Schmidt, *J. Polym. Sci. B*,**5**, 619 (1967).
[6] R. Hosemann, A. Schönfeld and W. Wilke, *Advances in Structure Research by Diffraction Methods*, Vol. III, p 101. Pergamon: Oxford; Friedr. Vieweg: Braunschweig (1970).
[7] A. J. Renouprez, *Diffusion des rayons X aux petits angles*, International Union of Crystallography, *Bibliography* 4 (1970).
[8] R. Hosemann and S. N. Bagchi, *Direct Analysis of Diffraction by Matter*, North Holland: Amsterdam (1962).
[9] P. Debye and A. M. Bueche, *J. Appl. Phys.* **20**, 518 (1949).
P. Debye, H. R. Anderson and H. Brumberger, *J. Appl. Phys.* **28**, 679 (1957).
[10] G. Porod, *Kolloidzschr.* **124**, 83 (1951).
[11] G. R. Strobl, *Acta Cryst. Camb.* **A26**, 367 (1970).
[12] H. G. Kilian, *Faserforschg. u. Textiltechnik*, **11**, 23 (1963).
W. Glenz, H. G. Kilian und F. H. Müller, *Kolloid-Z.u.Z.f. Polym.* **206**, 104 (1965).

[13] E. W. Fischer, F. Kloos and G. Lieser, *J. Polym. Sci.* **B7**, 845 (1969).
[14] A. Nobuta, A. Chiba and M. Kaneko, *Rep. Progr. Polym. Phys. Japan*, **12**, 137 (1969).
[15] E. W. Fischer and F. Kloos, *J. Polym. Sci.* **B8**, 685 (1970).
[16] P. R. Swan, *J. Polym. Sci.* **42**, 525 (1960).
[17] F. C. Stehling and L. Mandelkern, *Macromolecules*, **3**, 242 (1970).
[18] A. Keller, *Rep. Progr. Phys.* **31**, 623 (1968).
[19] P. J. Flory, *J. Am. Chem. Soc.* **84**, 2857 (1962).
[20] F. Danusso, *Polymer, London*, **8**, 281 (1967).
[21] T. Tatsumi, T. Fukushima, K. Imada and M. Takayanagi, *J. Macromol. Sci.-Phys.* **B1**, 459 (1967).
[22] R. Zannetti, E. R. Ferracini and G. Celotti, *Chim. e Industr.* **49**, 1060 (1967).
[23] C. Geacintov, R. B. Miles and H. J. L. Schuurmans, *J. Polym. Sci.* **C14**, 283 (1966).
[24] G. Lieser and E. W. Fischer, unpublished results.
[25] A. Keller and A. O'Connor, *Disc. Faraday Soc.* **25**, 114 (1958).
[26] W. O. Statton and P. H. Geil, *J. Appl. Polym. Sci.* **3**, 357 (1960).
[27] E. W. Fischer, *Kolloid-Z. u.Z.f. Polym.* **231**, 458 (1969).
[28] E. W. Fischer, H. Goddar and G. F. Schmidt, *Makromol. Chem.* **118**, 144 (1968).
[29] G. R. Strobl, *Dissertation*, Mainz (1970).
[30] E. W. Fischer, K. Malzahn, G. R. Strobl and I. Voigt-Martin, unpublished results.
[31] J. D. Hoffman, *Kolloid-Z. u.Z.f. Polym.* **231**, 499 (1969).
[32] P. K. Sullivan and J. J. Weeks, *J. Res. Nat. Bur. Stand.* **74A**, 203 (1970).
[33] Y. Nukushina, Y. Itoh and E. W. Fischer, *Polymer Letters*, **3**, 383 (1965).
[34] S. Blasenbrey and W. Pechhold, *Rheologica Acta*, **6**, 174 (1967).
[35] S. Blasenbrey, *Dissertation*, Stuttgart (1966).
[36] M. G. Broadhurst, *J. Res. Nat. Bur. Stand.* **66A**, 241 (1962).
[37] S. M. Ohlberg, *J. Phys. Chem.* **63**, 248 (1959).
[38] C. M. L. Atkinson and M. J. Richardson, *Trans. Faraday Soc.* **65**, 1749 (1969).
[39] A. Keller, *Phil. Mag.* **6**, 329 (1961).
[40] F. J. Balta Calleja, D. C. Bassett and A. Keller, *Polymer, London*, **4**, 269 (1963).
[41] P. J. Flory and A. Vrij, *J. Am. Chem. Soc.* **85**, 3548 (1963).
[42] L. A. Wood and N. Bekkedahl, *J. Appl. Phys.* **17**, 362 (1946).
[43] H. Wilski, unpublished results.
[44] P. Holdsworth and E. W. Fischer, unpublished results.
[45] E. W. Fischer and H. Hespe, *Kolloid-Z. u.Z.f. Polym.* **231**, 558 (1969).
[46] P. J. Flory, *Trans. Faraday Soc.* **51**, 848 (1955).
[47] J. M. Schultz, W. H. Robinson and G. M. Pound, *J. Polym. Sci.* **A2**, 511 (1967).
[48] Yu. A. Zubor and D. Ya. Tsvankin, *Vysokomol. Soedin.* 7, 1848 (1965).
[49] J. V. Dawkins, P. J. Holdsworth and A. Keller, *Makromol. Chem.* **118**, 361 (1968).
[50] K. O'Leary and P. H. Geil, *J. Macromol. Sci.* **B1**, 147 (1967).
[51] R. Zannetti, A. Fichera, G. Celotti and A. F. Martelli, *Europ. Polym. J.* **4**, 399 (1968).
[52] M. Kurokawa, *Rep. Univ. Fukuj., Eng. Fac.* **11**, 23 (1962).
[53] M. Shimomura, A. Chiba and J. Furuichi, *Rep. Progr. Polym. Phys. Japan*, **9**, 187 (1966); **10**, 147 (1967).
[54] E. W. Fischer, R. Martin, G. F. Schmidt and G. R. Strobl, Preprint IUPAC Symposium Toronto (September 1968).
[55] E. W. Fischer and Ch. Fritzsche, unpublished results.
[56] G. F. Schmidt, unpublished results.
[57] E. W. Fischer and D. Reuße, unpublished results.
[58] C. G. Vonk and G. Kortleve, *Kolloid-Z. u.Z.f. Polym.* **220**, 19 (1967).
[59] E. W. Fischer and G. F. Schmidt, *Angew. Chem., Internat. Ed.* **1**, 488 (1962).
[60] E. W. Fischer, *Kolloid-Z. u.Z.f. Polym.* **218**, 97 (1967).
[61] H. G. Zachmann, *Z. Naturforsch.* **19a**, 1397 (1964); **20a**, 719 (1965).
H. G. Zachmann and P. Spellucci, *Kolloid-Z. u.Z.f. Polym.* **213**, 39 (1966).
H. G. Zachmann, *Kolloid-Z. u.Z.f. Polym.* **216/217**, 180 (1967).
H. G. Zachmann and A. Peterlin, *J. Macromol. Sci.-Phys.* **B3**, 495 (1969).
[62] H. G. Zachmann, *Kolloid-Z. u.Z.f. Polym.* **231**, 504 (1969).